# We are IntechOpen,
# the world's leading publisher of
# Open Access books
# Built by scientists, for scientists

## 5,000
Open access books available

## 125,000
International authors and editors

## 140M
Downloads

Our authors are among the

## 154
Countries delivered to

## TOP 1%
most cited scientists

## 12.2%
Contributors from top 500 universities

CLARIVATE ANALYTICS
**BOOK CITATION INDEX**
INDEXED

**WEB OF SCIENCE**™

Selection of our books indexed in the Book Citation Index
in Web of Science™ Core Collection (BKCI)

## Interested in publishing with us?
## Contact book.department@intechopen.com

Numbers displayed above are based on latest data collected.
For more information visit www.intechopen.com

# Surface Chemical Analysis of Solid-Electrolyte Interphase Layer on Germanium Thin Films and the Effect of Vinylene Carbonate Electrolyte Additive

*Silpasree S. Jayasree, Shantikumar Nair*
*and Dhamodaran Santhanagopalan*

## Abstract

Germanium thin-film anodes for Li-ion battery applications are the focus of the present work. As part of this chapter, we shall briefly review the use of germanium thin films in Li-ion batteries, and subsequently, new results pertaining to the effect of vinylene carbonate (VC) as electrolyte additive on the electrochemical performance are presented. We have used cyclic voltammetry, galvanostatic charge-discharge and electrochemical impedance spectroscopy to investigate the performance. Thin-film electrode performance with 0 wt. %, 5 wt. %, and 10 wt.% VC as electrolyte additive was compared to understand the role of additive's concentration. The cell with 5 wt.% VC as electrolyte additive exhibited best performance with high specific capacity of 975 mAh/g, with a retention of 94 and 99% Coulombic efficiency at the end of 100 cycles. Ex situ surface chemical analysis of the solid-electrolyte interphase (SEI) layer has been studied in detail using X-ray photoelectron spectroscopy and correlated with the electrochemical performance.

**Keywords:** surface chemistry, SEI layer, germanium thin films, electrolyte additives, vinylene carbonate

## 1. Introduction

With the ever-increasing demand for energy and storage, the need for lithium-ion batteries (LIB) with more safety, high-energy density, power density, and miniaturized size has become critical. Studies have focused on the development of new potential anode materials that could substitute for the commercialized graphite [1, 2]. The group (IV) elements (silicon, germanium, tin) undergoing the mechanism of alloying with lithium have gained attention owing to their high theoretical capacities (4200, 1600, and 994 mAh/g, respectively). Alloying materials have low working potential compared to that of conversion and most of the insertion metal oxides, which is the key parameter for high-energy density full-cell applications [3–5]. Among group (IV) elements, the Li-Si system gained attention for its large

gravimetric capacity. High-power application of Si anode is bottlenecked by the huge volume expansion (>300%) associated with alloying/dealloying and by the slow lithium-ion transport. Pulverization of electrodes and crack formation on the active layer leads to rapid capacity fading and poor rate capability over cycling [6–8].

Germanium has gained attention despite its high cost. It offers a high theoretical capacity of 1384 mAh/g ($Li_{15}Ge_4$) with improved kinetics, and it also possesses a volumetric capacity almost equal to Si (7366 Ah/L for $Li_{15}Ge_4$ and 8334 Ah/L for $Li_{15}Si_4$). Lithium-ion diffusivity is higher in Ge, i.e., ~400 times the diffusivity in Si at room temperature, and germanium exhibits $10^4$ times higher electrical conductivity than Si [9–11].

Despite of all these attractive advantages, Ge has a few limitations that hinder its commercialization. Some unwanted side reactions between active material and electrolyte result in solid-electrolyte interphase (SEI) layer formation that comprises of lithium carbonates, lithium alkoxides, etc. The pulverization of material occurring due to the drastic volume change during charge/discharge generates an unstable SEI layer on electrode surface, and it also has been reported that diffusion length gets increased because of the aggregation of active particles. This results in increased cell impedance and attenuation of capacity and Coulombic efficiency [12, 13].

Many strategies have been adopted so far to minimize the volume expansion and to improve the electrochemical performance. Nanoscale Ge is considered as an effective method compared to bulk Ge because of the low volume expansion and less aggregation of materials. Increased surface area in nanoscale enhances the ion transport at the electrode/electrolyte interface and also decreases the diffusion length. Several groups investigated and reported the increased performance of Ge nanoparticles [13], nanocrystals [3], nanowires [2], and nanotubes [14] compared to bulk. The importance of surface coating (<1 μm) and alloy formation has been reported by some groups [11]. It shows a reduction in volume expansion and increased electrochemical performance. Fabrication and implementation of Ge thin films (<250 nm thickness) can be treated as a promising solution for attaining stability, rate capability, and long life cycle because of its low volume expansion. Studies reported the improved performance of Ge films in terms of rate capability, electronic and ionic conductivity, retention, etc. [15, 16]. Silicon thin-film electrodes suffer crack formation and loss of electrical contact with the current collector. In contrast, even though crack formation occurs on the surface of the germanium electrode, no lack of electrical contact between material and current collector was observed and hence resulted in superior rate capability of Ge thin films [17]. Electrolyte additives accentuate the electrochemical performance. Vinylene carbonate (VC), fluoroethylene carbonate (FEC), vinyl ethylene carbonate (VEC), etc. are the commonly used additives. These additives will reduce and form stable layer on the electrode surface at a high potential. The surface layer thus formed will allow Li-ion transport through it and inhibit further electrolyte decomposition. SEI layer components depend on the functional groups present in the additive [18, 19].

Herein, we report the fabrication of Ge thin films by thermal evaporation process and study of its structural and electrochemical properties with/without the electrolyte additive, VC. Surface chemical analysis of SEI layer formation on Ge thin films was evaluated in detail to correlate with the electrochemical cycling stability.

## 2. Brief review on germanium thin-film-based Li-ion battery electrodes

Many groups had studied and reported the potential of germanium thin films as anode for LIB applications. Films were developed via thermal evaporation [6, 12, 17],

electron-beam evaporation [8, 15, 16, 20], sputtering [21–24], electrodeposition [25], and alloying [26–28].

Graetz et al. [6] did a comparative study between Ge nanocrystals (12 nm mean diameter) and amorphous thin films (60–250 nm thickness) as anodes for LIB. Nanocrystals were obtained by ballistic deposition, and amorphous film fabrication was done via thermal evaporation. In Ge nanocrystals, different Li-Ge crystalline phases were formed upon lithiation that ended up with severe capacity loss after a few cycles. It is because of the material decrepitating caused by increased stress during cycling. In case of a-Ge thin film, partition of film occurs due to the crack formation and propagation. These island-like partitions accommodate the volume change during cycling, ensuring proper electric contact between substrate and material. Upon lithiation, a-Ge became crystalline, and it remains as such during further delithiation. It delivered a capacity of 1.7 Ah/g over 62 cycles without any capacity loss, whereas Ge nanocrystals exhibited a capacity of 1.4 Ah/g with 60% retention at the end of 50 cycles. Thin-film electrodes showed rate capability up to 1000 C with very less reduction in capacity. They suggest that the absence of defects, increased surface area, and reduction in diffusion length resulted in enhanced performance of a-Ge thin films.

Germanium thin films were fabricated and coupled with single wall carbon nanotube (SWCNT) that acts as current collector. Dileo et al. [8] introduced a method to increase energy density of battery by the removal of inactive current collectors. They deposited Ge on SWCNT via electron-beam evaporation with different loadings of 10, 20, and 40%. Ge-SWCNT with 40 wt.% Ge exhibited an increased capacity of 800 mAh/g. Full cells were developed with 40 wt.% Ge-SWCNT as anode and commercialized $LiCoO_2$ as cathode, also used mesocarbon microbead (MCMB) as anode for comparison. Ge-SWCNT/$LiCoO_2$ full cell maintained a constant discharge voltage of 3.35 V. Ge-SWCNT showed an improved anode energy density of 1600 Wh/kg compared to MCMB (670 Wh/kg).

Bagetto et al. [17] presented the electrochemical and in situ X-ray diffraction study of Ge thin films for the better understanding of Li-ion insertion/deinsertion mechanism. Upon complete lithiation, both the electrodes got transformed to crystalline $Li_{15}Ge_4$ leading to maximum storage capacity for the specified composition. The rate capability test on evaporated films was conducted during delithiation. It was discharged from 0.1C to a high rate of 100C. Eve at 100C, it delivered high capacity that indicates the proper Li diffusion into the evaporated Ge films. Insertion reaction was similar in both the films, whereas during deinsertion they observed a slight difference in the peak position. They were not able to point a proper reason for the difference in reaction of Li with both the films, hence recommended the need of further investigations. Impedance analysis and electrochemical equilibrium revealed the potential of evaporated films as a promising anode material than sputtered one.

Investigation on Ge thin films developed via radio frequency magnetron sputtering was done by Laforge et al. [21]. Doped and non-doped Ge targets were used for the deposition. Effect of doping concentration and electrode thickness was reported in detail. Non-doped, n-doped, and p-doped Ge films with different thickness of 50, 100, 200, and 400 nm were studied. The capacity of non-doped sample decreased rapidly at high current densities compared to doped films. Also the conductivity of non-doped samples (>1.25 mS/cm) was too low. The n-doped Ge films showed best conductivity of 30 mS/cm, whereas p-doped only had 5 mS/cm. This increased the life cycle of n-doped films compared to p-doped and non-doped. They prepared electrodes with different thickness of 50, 100, 200, and 400 nm. The n-doped Ge film of thickness 200 nm exhibited best life cycle among others. It showed a stable discharge capacity of 780 µAhcm$^2$/cm over 180 cycles.

In this work, they opened up the future scope for Ge as an eminent anode for thin-film battery applications.

Liu et al. [25] studied and reported the electrochemical performance of macroporous germanium thin films developed by electrodeposition from ionic liquid. They did a comparative study between dense Ge and 3D-ordered macroporous (3DOM) films. 3DOM electrodes exhibited an improved rate performance and better life cycle compared to the other. At the end of 50 cycles, 3DOM film delivered a capacity of 844 mAh/g at 0.2C, whereas dense Ge film was only able to have a lithium storage of 611 mAh/g. Cracks formed on electrode surface of dense film led to pulverization of electrode and ended up in poor performance. Due to the porous structure of 3DOM, there was no crack formation. It played a role for minimizing the volume expansion and also increased the Li-ion diffusion pathways.

Abel et al. [27] reported the improved electrochemical performance of nanocolumnar $Ge_{0.9}Se_{0.1}$ electrodes prepared via vacuum deposition. They did an investigation on Se-free and Se-alloyed Ge as anode. The addition of Se to nanocolumnar-structured Ge increased its Li-ion transport and thereby high rate performance. A film with a thickness of 100 nm got completely delithiated in a very short time of 5 s. Cells were highly stable over 1000 cycles at a rate of 61 A/g with a retention of 70%. At 1342 A/g, it exhibited a capacity of 940 mAh/g with 75% retention. It is clear from the TEM images that during the first cycle, there formed a Li-Se high ionic conducting phase in the material that paved way for the enhanced performance.

## 3. Structural, morphological, and electrochemical results of thermally evaporated germanium thin films

### 3.1 Experimental

The deposition of thin-films was carried out in a cluster tool deposition system installed in the lab (**Figure 1** shows the photograph of the system). The cluster tool system is equipped with multiprocess chambers (including DC, RF-magnetron sputtering, and thermal evaporation) connected through load-lock and transfer chamber separated by gate valves (for independent operation). The system is equipped to transfer samples from one process chamber to the other using magnetic transfer arms without atmospheric exposure of the samples. All the process chambers are equipped with turbo-molecular pump and a roughing
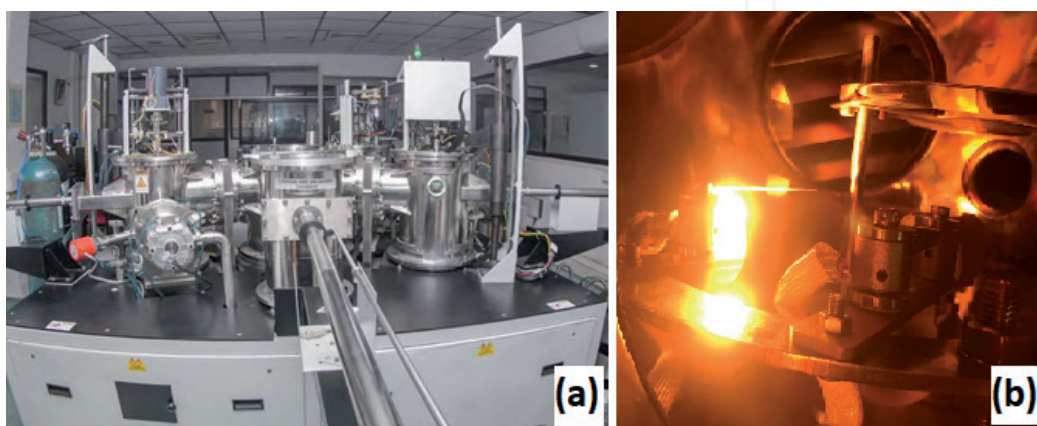


**Figure 1.**
*(a) Physical vapor deposition system installed in the lab and (b) thermal evaporation chamber view during operation.*

pump. For the present work, germanium thin films were deposited at room temperature on copper foil via thermal evaporation process with Ge granules as a source thermally evaporated from moly boat. Thermal evaporation chamber is loaded with a $5 \times 5$ cm$^2$ Cu foil (substrate) and pumped to a base vacuum of $5 \times 10^{-7}$ mbar prior to the evaporation process. The thermal evaporator uses a power supply of 200 A and 10 V maximum. Once the base vacuum is attained, the current was gradually increased from 0 to 70 A, and the germanium granules were allowed to completely evaporate at 70 A by maintaining the same for a few minutes. During deposition the substrate holder was rotated at 10 rpm to ensure uniformity over the area of deposition. The deposited films underwent structural and morphological characterization as well as electrochemical analysis. X-ray diffraction of the resultant films was obtained from Cu Kα X-rays (Bruker AXS D8 Advance, Germany). Cross-section image was recorded using JSM 6490 (JEOL, Japan) scanning electron microscopy (SEM), while the surface images were recorded using JSM 7610FPlus (JEOL, Japan) field emission SEM microscope. Raman spectrum was collected using a 633 nm diode laser (Witech Alpha 300R, Germany). Surface analysis of the films was carried out with Axis Ultra spectrometer (Kartos, UK) with monochromated Al-K$_\alpha$ as X-ray source. The spectra obtained were calibrated based on C 1S peak at 284.6 eV. Galvanostatic charge-discharge performances were studied at room temperature using electrochemical workstation (Biologic Instruments, USA) with a voltage range of 0.01–2 V. Ge films deposited on Cu foil were cut into small pieces with a loading of 63 µg/cm$^2$ for electrochemical testing in coin cells (CR 2032) crimped inside the argon-filled glovebox maintained with O$_2$ and H$_2$O levels <1.0 ppm (UNIlab Pro, MBRAUN, Germany). Lithium foil was used as counter electrode with glass microfibers (GF/D, Whatman) as separators and 1 M LiPF$_6$ dissolved in EC: DMC (1:1 vol. %) as electrolyte (PuriEL, Canada). VC additive electrolytes were prepared in glovebox by adding 5 and 10 wt.% of VC to the electrolyte under stirring for a few minutes. Cycled electrodes (100 cycles) were washed in dimethyl carbonate (DMC) and dried in the glovebox before the surface chemical analysis.

## 3.2 Structural and morphological analysis

**Figure 2a** shows the XRD pattern of the deposited Ge films. It is shown that the films obtained are crystalline in nature. Characteristic peaks of Ge were located at 26.97°, 45.2°, and 54.8° that correspond to 111, 220, and 311, respectively [13]; small
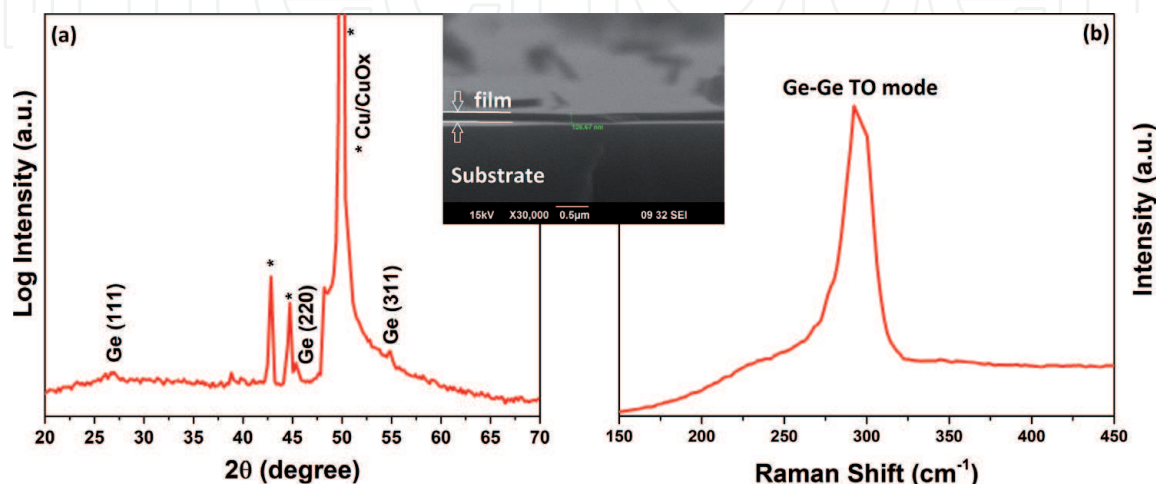


**Figure 2.**
*(a) XRD of Ge film deposited on Cu-foil and (b) Raman spectrum of prepared Ge film. Inset shows the cross sectional SEM image of the Ge film.*

shift in the peak positions could be due to strain effects. The presence of $Cu/CuO_x$ (substrate) peaks is indexed in the figure [29]. Raman spectrum of Ge films with a peak at 292 cm$^{-1}$ is depicted in **Figure 2b**, which represents the Ge-Ge transverse optical phonon mode. The sharp and intense peak confirms the local structural ordering of the film [22], while a small shift to lower frequency may be due to the strain effect. Inset in **Figure 2** displays the cross-sectional SEM image of Ge film which clearly shows Ge layer thickness of about 125 nm. It also reveals the high-thickness uniformity of the deposited thin film.

## 3.3 Electrochemical results

The additive concentration was varied, and sample identifications are based on the weight percentage of the additive, 0 wt.% VC (without additive), 5 wt.% VC and 10 wt.% VC Ge electrodes, respectively. For the understanding of electrochemical redox potentials of the deposited films, cyclic voltammetry was done at a scan rate of 0.1 mV/s in a voltage window of 0–1.2 V and is shown in **Figure 3**. **Figure 3a–c** corresponds to the 0 wt.% VC electrode, 5 wt.% VC, and 10 wt.% VC Ge electrodes, respectively. It is seen that for all three samples, there is a strong oxidation peak at 0.53 V due to the delithiation process. Reduction peaks were observed at 0.05, 0.14, 0.31, and 0.38 V that attributes to Li-Ge alloy formation [3, 15]. In second and third cycle, two reduction peaks got shifted to 0.38 and 0.50 V for all three electrodes. Structural modifications happened during the first lithiation which contributes to the peak shift in further cycles. Oxidation and reduction peaks are well superimposed for all, which reveals the reversibility of the films.
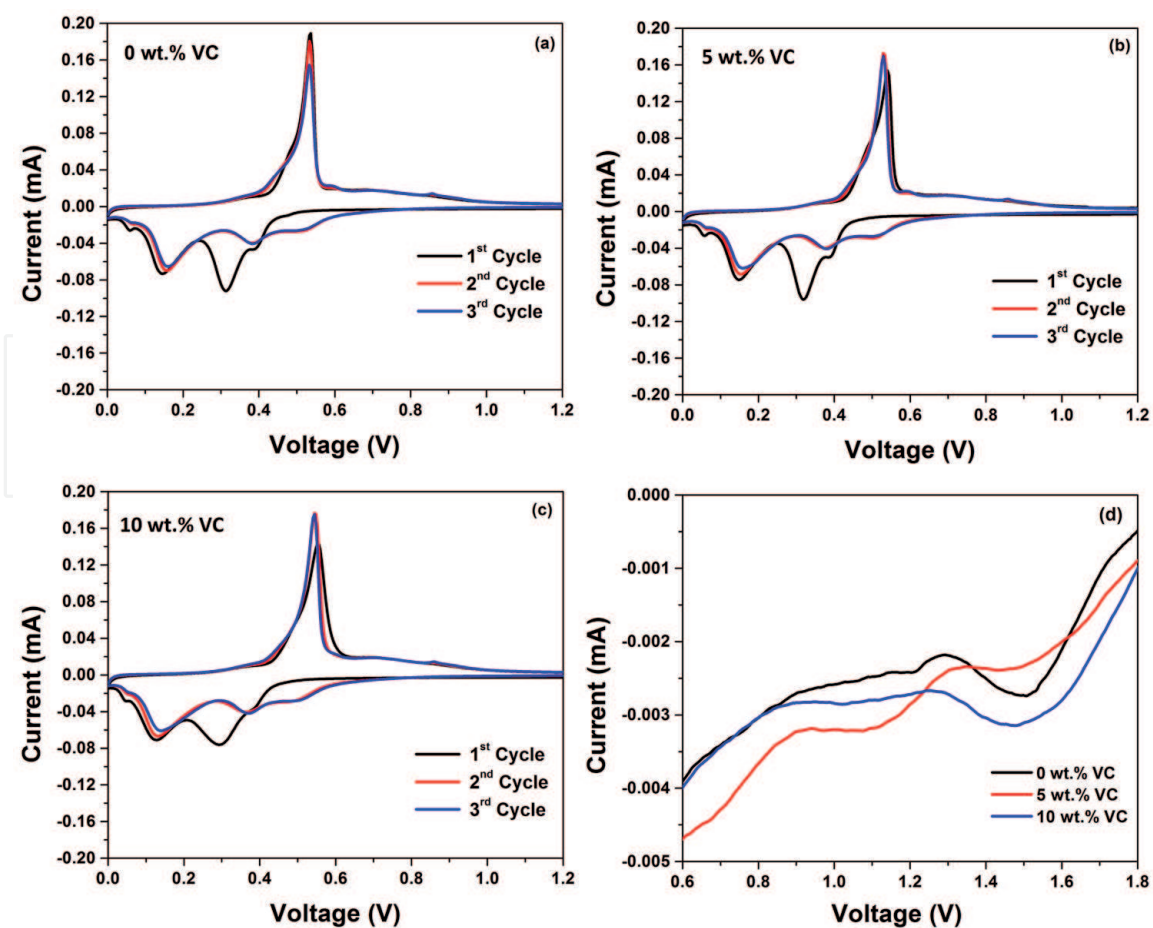


**Figure 3.**
*Cyclic voltammogram of Ge films (a) without electrolyte additive (b) with 5 wt.% VC (c) with 10 wt.% VC and (d) first cycle reduction peaks of 0 wt.%, 5 wt.% and 10 wt.% VC samples in a voltage range of 0.6–1.8 V.*

The first cycle reduction peaks of all the three samples in a voltage range of 0.6–1.8 V were shown in **Figure 3d**. The presence of peaks at 1.05 and 1.02 V in 5 wt. % and 10 wt.% VC films, respectively, is attributed to the reduction of VC [3]. 0 wt. %, 5 wt. %, and 10 wt.% VC films showed a reduction peak at 1.5 V. It may be due to the presence of SEI layer formed from surface oxides. Reduction of VC in 5 wt.% VC Ge film formed a stable layer on electrode/electrolyte interface that prevented it from further electrolyte decomposition which resulted in improved electrochemical performance.

Ge thin films were cycled at a current density of 1.6 A/g in a potential window of 0.01–2 V. **Figure 4a–c** shows the charge-discharge profiles of the germanium electrodes without and with electrolyte additives as indicated. **Figure 4d** depicts the life cycle of the material with and without using the electrolyte additive, VC. Ge electrodes with 5 wt.% VC and 10 wt.% VC show stable performance compared to the 0 wt.% VC. Unstable SEI layer formed on the electrode surface due to the electrolyte decomposition leads to capacity fade after a few cycles. It is seen that the 0 wt.% VC electrode delivered a capacity of 871 mAh/g after the first discharge and gradually capacity decreased to 386 mAh/g with only 50% retention at the end of 100 cycles. Cell with 5 wt.% VC as electrolyte additive showed improved capacity compared to that of 10 wt.% VC. A high initial capacity of 975 mAh/g with a retention of 94 and 99.4% Coulombic efficiency (CE) at the end of 100 cycles was recorded for the 5 wt.% electrode. Whereas for 10 wt.% VC as electrolyte additive, the electrode exhibited lower initial capacity of 778 mAh/g and a CE of 99.4% at the end of 100 cycles. At higher potential, VC got reduced and formed a stable layer on electrode/electrolyte interface that contains poly VC compounds. The layer formed has proper Li-ion conductivity and also prevents the electrolyte from decomposition. Improved performance of Ge electrode with 5 wt.% VC compared to 10 wt.% VC is attributed to the less amount of poly species formed on the electrode surface due to VC reduction.

Electrochemical impedance studies were done on 0 wt. % VC, 5 wt. % VC, and 10 wt.% VC electrodes for understanding the effect of electrolyte additive and is
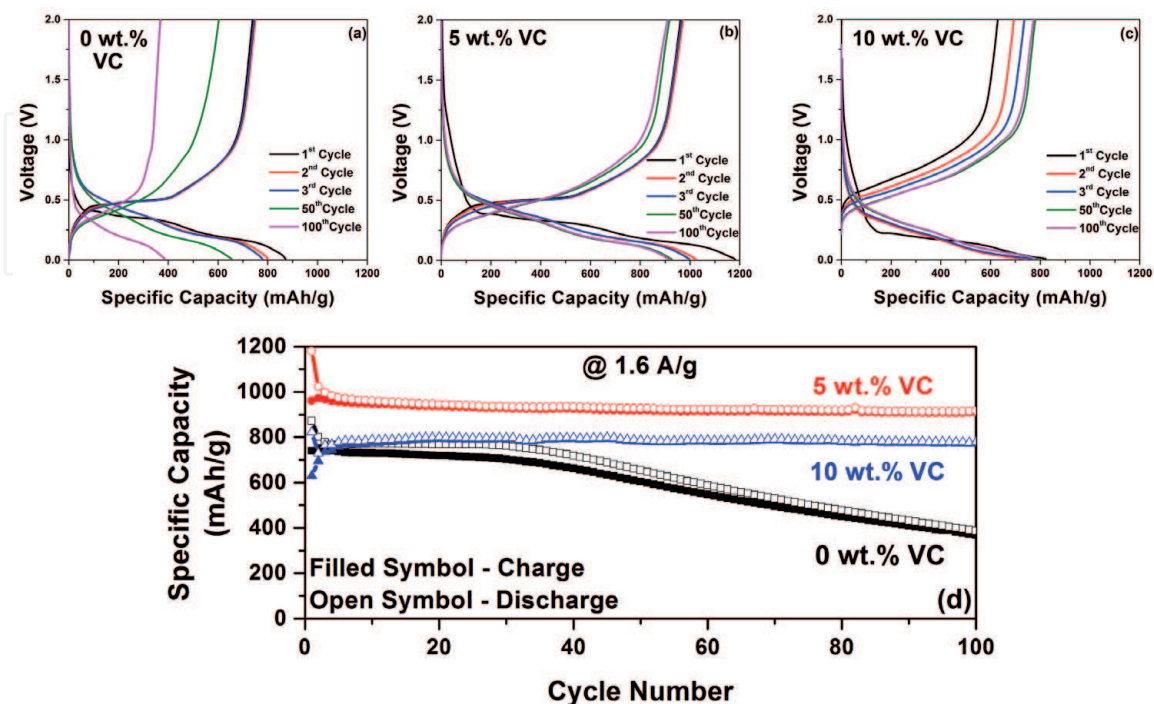


**Figure 4.**
*Charge-discharge profiles of (a) Ge with 0 wt.% VC (b) Ge with 5 wt.% VC and (c) Ge with 10 wt.% VC (d) Cycling data of Ge electrodes with and without electrolyte additive.*
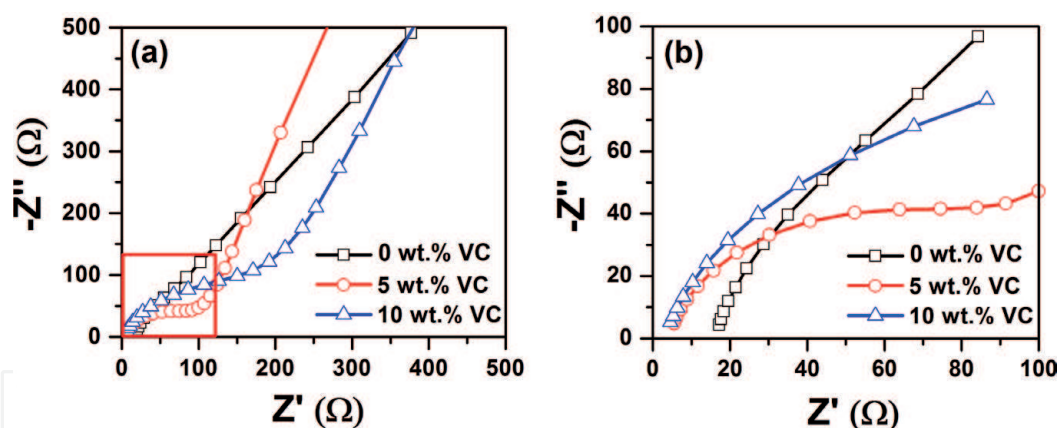
**Figure 5.**
*(a) Electrochemical impedance spectroscopy of Ge films at OCV condition and (b) enlarged view of the region marked in 5(a).*

illustrated in **Figure 5**. **Figure 5a** indicates the electrochemical impedance spectroscopy (EIS) results of the three electrodes. It is observed that except the 0 wt.% VC electrode, the electrodes with electrolyte additive show a depressed semicircle in the high-mid-frequency region followed by a straight line in the low-frequency region. 0 wt.% VC electrode shows only a straight line without any obvious semicircle indicating a capacitive charge storage with poor electronic conduction. The semicircle intersection with the x-axis at high frequency gives information about the series resistance, and information about charge-transfer resistance is given by the intersection at mid-frequency region. The slope of the straight line in the low-frequency region gives information about Li-diffusion kinetics. **Figure 5b** shows the closer view of high-frequency region marked in (a). Series resistance ($R_S$) value is high for 0 wt.% VC compared to 5 wt. % VC and 10 wt.% VC samples. It exhibits a $R_S$ value of 17.15, 5.46, and 4.54 $\Omega$ for 0 wt.% VC, 5 wt.%, and 10 wt.% VC samples, respectively. Charge-transfer resistance, $R_{ct}$ values of VC 5 wt.%, ad VC 10 wt.% electrodes were 106.0 and 237.8 $\Omega$, respectively, while the 0 wt.% VC electrode did not show any semicircle indicating infinite $R_{ct}$ value. Lower $R_s$ ad $R_{ct}$ values for the 5 wt.% VC additive electrode validate the improved electrochemical performance discussed above.

## 4. Surface chemical analysis of cycled germanium thin-film electrodes

In order to gain a clear insight on the solid-electrolyte interphase layer, surface chemical analysis was performed. XPS analysis were carried out on as-deposited as well as 0 wt.%, 5 wt.%, and 10 wt.% VC additive electrochemically cycled electrodes (in charged condition, after 100 cycles). **Figure 6a** shows the high-resolution spectra of C 1 s in which C-C peak at 284.65 eV which is common in all the samples. The numbers on the left side of the individual spectrum indicate the intensity multiplication factor for normalization. The presence of $CO_3$, C=O, and C-O were observed at 289.85, 288.05, and 286.75 eV, respectively, only in cycled electrodes due to electrolyte decomposition. Peak intensity of carbonates is less in 5 wt.% electrode compared with 0 wt. % VC and 10 wt.% VC sample. C-Ge peak at 282.75 eV is seen only in 0 wt.% VC sample, which implies the SEI layer formation during cycling owing to the unwanted side reactions. **Figure 6b** shows the O 1S spectra of the films having $OH^-$ peak at 532.25 eV only for the as-deposited sample, whereas $GeO_x$ is present in all the four samples at 531.45 eV. The intensity of $GeO_x$ peak is high in cycled electrodes compared with the as-deposited. Li 1 s spectra are shown in
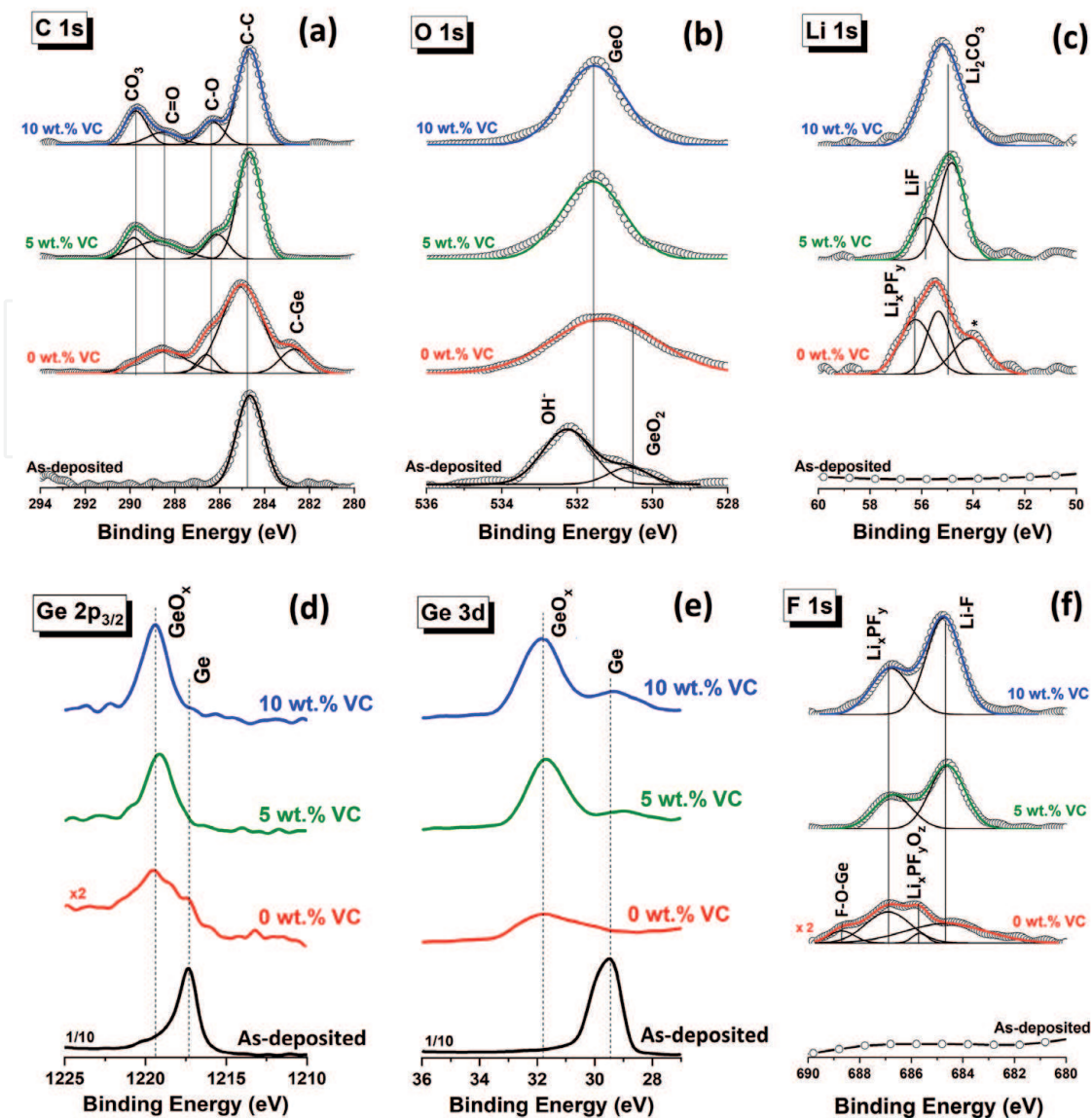
**Figure 6.**
*High resolution XPS spectra of (a) C 1s, (b) O 1s, (c) Li 1s, (d) Ge 2p, (e) Ge 3d and (f) F 1s of as-deposited Ge film and cycled electrodes with 0 wt.%, 5 wt.% and 10 wt.% VC.*

**Figure 6c** indicating the presence of LiF and $Li_2CO_3$ at 55.95 and 54.95 eV, respectively, except for the as-deposited sample. This may be from the SEI layer formed on the surface of the electrodes due to the decomposition of electrolyte at low voltages. It is seen that the amount of $Li_2CO_3$ is high in 10 wt.% VC electrode compared with 0 wt. % VC and 5 wt.% VC electrode. Peaks at 1219.35 and 1217.35 eV shown in **Figure 6d** correspond to $GeO_x$ and Ge, respectively. In as-deposited sample, Ge exists only in its elemental form. However, Ge is mostly observed to be as $GeO_x$ in cycled electrodes. It is indeed important to note that the Ge peak shoulder was for the 0 wt.% VC electrode in Ge $2p_{3/2}$. It is believed to be due to the effect of noise and signal fluctuation as the intensity for the whole spectrum was too low (the intensity reported for this electrode is multiplied by a factor of 2 as indicated in the figure). In general, Ge 3d is preferable over Ge 2p if Ge concentration is low or if it is expected to be a buried layer. Ge 3d electrons are capable of penetrating from buried layer compared to that of Ge 2p electrons due to its higher kinetic energy. This can be further verified by recording the high-resolution spectra in Ge 3d region. **Figure 6e** shows the high-resolution Ge 3d spectra with Ge and $GeO_x$ peaks observed at 31.75 and 29.45 eV, respectively. The presence of Ge peak for the electrodes cycled with VC electrolyte additive indicates a thin SEI layer. In 0 wt.% VC electrode, only
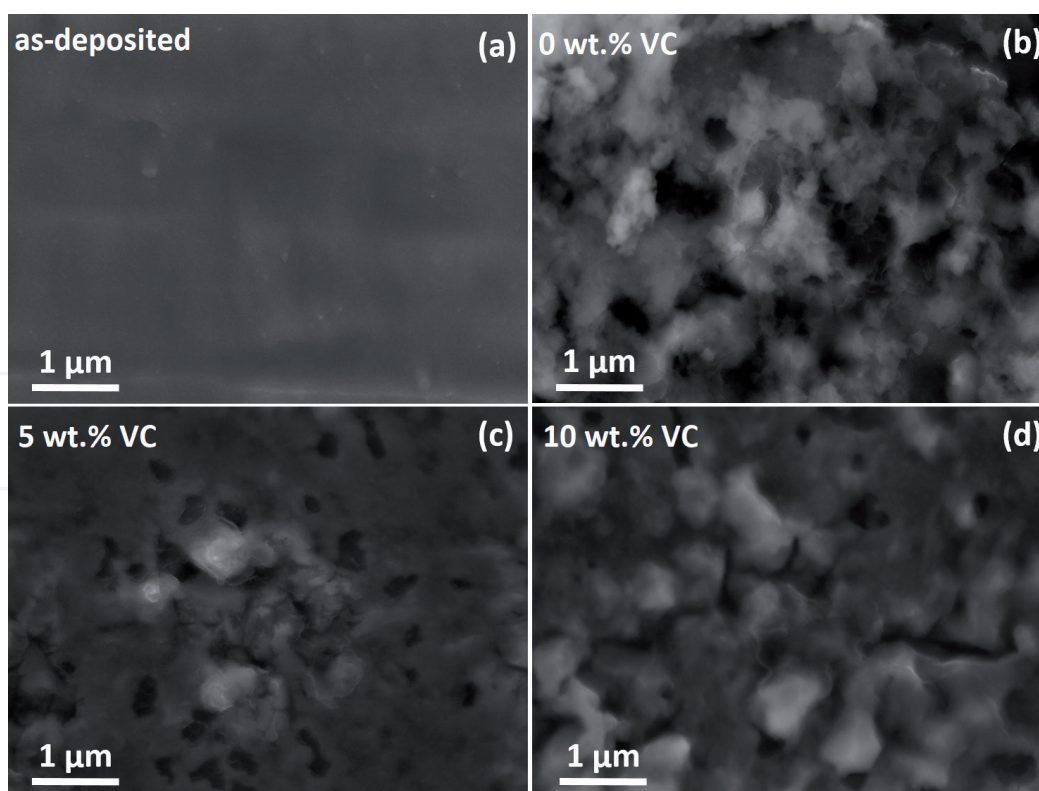
**Figure 7.**
*FESEM images of the electrodes surface for (a) as-deposited Ge film, cycled electrodes with (b) 0 wt.%, (c) 5 wt.% and (d) 10 wt.% VC.*

the presence of $GeO_x$ is observed, which can be attributed to the thicker SEI layer formed by electrolyte decomposition during the cycling of electrodes [19]. Also Ge 3d seems to be more sensitive to elemental germanium than Ge 2p as observed from its intensity. The 5 wt.% and 10 wt.% VC electrodes have both Ge and $GeO_x$ peaks that indicates thinner and stable SEI layer. The intensity of oxide peak is high in 10 wt.% VC electrode [30, 31]. F 1 s spectra is given in **Figure 6f** which depicts the presence of LiF, $Li_xPF_yO_z$, and $Li_xPF_y$ at 684.8, 685.7, and 686.9 eV, respectively [32]. As expected, these peaks are absent in as-deposited sample. The presence of LiF and $Li_xPF_y$ is seen more in 10 wt.% VC electrode, while a small amount of F-O-Ge (~688.6 eV) and $Li_xPF_yO_z$ are observed in 0 wt.% electrode only. Increased amount of LiF, $Li_2CO_3$, and $GeO_2$ in 10 wt.% VC electrode can act as an insulating layer for Li-ion diffusion that attenuates the electrochemical performance compared with 5 wt.% VC electrode. Further to investigate the surface morphology of the as-deposited and cycled electrodes (after 100 cycles), SEM images were recorded; **Figure 7** shows the SEM images of as-deposited, 0 wt. % VC, 5 wt. % VC, and 10 wt.% VC electrodes. As-deposited films have smooth, pore-free, and crack-free surface. It is observed that carbon-rich SEI layer along with pores and cracks have been formed on the surface of 0 wt.% VC electrode compared to the other two electrodes, while 10 wt.% VC electrode showed more porous and cracked surface compared to 5 wt.% VC electrode. This along with the XPS analysis indicates that 5 wt.% VC electrode high-performance anode is well correlated with the thin and stable SEI layer.

## 5. Conclusions

Ge thin-film anodes were developed via thermal evaporation process for LIB applications. Structural analysis revealed the crystalline nature of the deposited Ge film. The effect of VC as electrolyte additive and its concentration on

electrochemical cycling stability were studied in detail. Galvanostatic charge-discharge studies showed best performance for 5 wt.% VC compared to that of 0 and 10 wt.% VC. It exhibited a high initial capacity of 975 mAh/g with a retention of 94 and 99% Coulombic efficiency at the end of 100 cycles. Cyclic voltammetry clearly showed the reduction of VC at 1.05 V in 5 wt.% additive sample that led to the formation of a stable and thin SEI layer on the film surface which prevented further electrolyte decomposition. This is attributed to the low-series and charge-transfer resistance values for 5 wt.% VC additive. Improved electrochemical performance of the electrode cycled with 5 wt.% VC was correlated with the surface chemical analysis of solid-electrolyte interphase layer. XPS results confirmed that the SEI layer had a mixed organic and inorganic composition for all the electrodes. The SEI layer composition with VC as electrolyte additive had LiF as a major component and significant amount of $Li_xPF_y$; in contrary, it was $Li_xPF_yO_z$ and negligible LiF for the electrode without VC additive. The presence of $Li_2CO_3$ in all the electrodes indicated that it played a least significant role in the performance. The surface SEM images of the cycled electrodes were consistent with the electrochemical performance and its correlation with the XPS results.

## Acknowledgements

## Conflict of interest

The authors declare no conflict of interest.

## Author details

Silpasree S. Jayasree, Shantikumar Nair and Dhamodaran Santhanagopalan*
Centre for Nanosciences and Molecular Medicine, Amrita Vishwa Vidyapeetham, AIMS, Kochi, Kerala, India

*Address all correspondence to: dsgopalan20710@aims.amrita.edu

IntechOpen

## References

[1] Bogart TD, Chockla AM, Korgel BA. High capacity lithium ion battery anodes of silicon and germanium. Current Opinion in Chemical Engineering. 2013;**2**:286-293. DOI: 10.1016/j.coche.2013.07.001

[2] Chan CK, Zhang XF, Cui Y. High capacity Li ion battery anodes using Ge nanowires. Nano Letters. 2008;**8**:307-309. DOI: 10.1021/nl0727157

[3] Gulzar U, Li T, Bai X, Goriparti S. Nitrogen-doped single walled carbon nanohorns enabling effective utilization of Ge nanocrystals for next generation lithium ion batteries. Electrochimica Acta. 2018;**298**:89-96. DOI: 10.1016/j.electacta.2018.11.130

[4] Tian H, Xin F, Wang X. High capacity group-IV elements (Si, Ge, Sn) based anodes for lithium-ion batteries. Journal of Materiomics. 2015;**1**:153-169. DOI: 10.1016/j.jmat.2015.06.002

[5] Chen L, Wang K, Xie X. Effect of vinylene carbonate (VC) as electrolyte additive on electrochemical performance of Si film anode for lithium ion batteries. Journal of Power Sources. 2007;**174**:538-543. DOI: 10.1016/j.jpowsour.2007.06.149

[6] Graetz J, Ahn CC, Yazami R. Nanocrystalline and thin film germanium electrodes with high lithium capacity and high rate capabilities. Journal of the Electrochemical Society. 2004;**151**:A698-A702. DOI: 10.1149/1.1697412

[7] Ocon JD, Lee KJ, Lee J. High energy density germanium anodes for next generation lithium ion batteries. Applied Chemical Engineering. 2014;**251**:1-13. DOI: 10.14478/ace.2014.1008

[8] DiLeo RA, Ganter MJ, Landi BJ. Germanium–single-wall carbon nanotube anodes for lithium ion batteries. Journal of Materials Research. 2010;**25**:1441-1446. DOI: 10.1557/JMR.2010.0184

[9] Yoon S, Park CM, Sohn HJ. Electrochemical characterizations of germanium and carbon-coated germanium composite anode for lithium-ion batteries. Electrochemical and Solid-State Letters. 2008;**11**:A42-A45. DOI: 10.1149/1.2836481

[10] Ren JG, Wu QH, Tang H. Germanium–graphene composite anode for high-energy lithium batteries with long cycle life. Journal of Materials Chemistry A. 2013;**1**:1821-1826. DOI: 10.1039/c2ta01286c

[11] Hu Z, Zhang S, Zhang C. High performance germanium-based anode materials. Coordination Chemistry Reviews. 2016;**326**:34-85. DOI: 10.1016/j.ccr.2016.08.002

[12] Yu Y, Yan C, Gu L. Three-dimensional (3D) bicontinuous Au/amorphous-Ge thin films as fast and high-capacity anodes for lithium-ion batteries. Advanced Energy Materials. 2013;**3**:281-285. DOI: 10.1002/aenm.201200496

[13] Liu X, Lin N, Cai W. Mesoporous germanium nanoparticles synthesized in molten zinc chloride at low temperature as a high-performance anode for lithium-ion batteries. Dalton Transactions. 2018;**47**:7402-7406. DOI: 10.1039/C8DT01060A

[14] Park MH, Cho Y, Kim K. Germanium nanotubes prepared by using the Kirkendall effect as anodes for high-rate lithium batteries. Angewandte Chemie, International Edition. 2011;**50**:9647-9650. DOI: 10.1002/anie.201103062

[15] Wang X, Susantyoko RA, Fan Y. Vertically aligned CNT-supported thick

Ge films as high-performance 3D anodes for lithium ion batteries. Small. 2014;**10**:2826-2829. DOI: 10.1002/smll.201400003

[16] Rudawski NG, Darby BL, Yates BR. Nanostructured ion beam-modified Ge films for high capacity Li ion battery anodes. Applied Physics Letters. 2012;**100**:083111. DOI: 10.1063/1.3689781

[17] Baggetto L, Notten PH. Lithium-ion (de) insertion reaction of germanium thin-film electrodes: An electrochemical and in situ XRD study. Journal of the Electrochemical Society. 2009;**156**:A169-A175. DOI: 10.1149/1.3055984

[18] Haregewoin AM, Wotango AS, Hwang BJ. Electrolyte additives for lithium ion battery electrodes: Progress and perspectives. Energy and Environmental Science. 2016;**9**:1955-1988. DOI: 10.1039/c6ee00123h

[19] Mishra K, Xu W, Engelhard MH. The effect of solvent on the capacity retention in a germanium anode for lithium ion batteries. Journal of Electrochemical Energy Conversion and Storage. 2018;**15**:041012. DOI: 10.1115/1.4039860

[20] Li X, Yang Z, Fu Y. Germanium anode with excellent lithium storage performance in a germanium/lithium–cobalt oxide lithium-ion battery. ACS Nano. 2015;**9**:1858-1867. DOI: 10.1021/nn506760p

[21] Laforge B, Levan-Jodin L, Salot R. Study of germanium as electrode in thin-film battery. Journal of the Electrochemical Society. 2008;**155**:A181-A188. DOI: 10.1149/1.2820666

[22] Hwang CM, Park JW. Electrochemical characterizations of multi-layer and composite silicon–germanium anodes for Li-ion batteries using magnetron sputtering. Journal of Power Sources. 2011;**196**:6772-6780. DOI: 10.1016/j.jpowsour.2010.10.061

[23] Susantyoko RA, Wang X, Sun L. Influences of annealing on lithium-ion storage performance of thick germanium film anodes. Nano Energy. 2015;**12**:521-527. DOI: 10.1016/j.nanoen.2015.01.024

[24] Al-Obeidi A, Kramer D, Mönig R. Mechanical stresses and crystallization of lithium phosphorous oxynitride-coated germanium electrodes during lithiation and delithiation. Journal of Power Sources. 2016;**306**:817-825. DOI: 10.1016/j.jpowsour.2015.12.057

[25] Liu X, Zhao J, Hao J. 3D ordered macroporous germanium fabricated by electrodeposition from an ionic liquid and its lithium storage properties. Journal of Materials Chemistry A. 2013;**1**:15076. DOI: 10.1039/c3ta12923c

[26] Abel PR, Chockla AM, Lin YM. Nanostructured $Si_{(1-x)}Ge_x$ for tunable thin film lithium-ion battery anodes. ACS Nano. 2013;**7**:2249-2257. DOI: 10.1021/nn3053632

[27] Abel PR, Klavetter KC, Heller A. Thin nanocolumnar $Ge_{0.9}Se_{0.1}$ films are rapidly lithiated/delithiated. The Journal of Physical Chemistry C. 2014;**118**:17407-17412. DOI: 10.1021/jp504327e

[28] Abel PR, Klavetter KC, Jarvis K. Sub-stoichiometric germanium sulfide thin-films as a high-rate lithium storage material. Journal of Materials Chemistry A. 2014;**2**:19011-19018. DOI: 10.1039/C4TA04496G

[29] Cheng SL, Chen MF. Fabrication, characterization, and kinetic study of vertical single-crystalline CuO nanowires on Si substrates. Nanoscale Research Letters. 2012;**7**:119. DOI: 10.1186/1556-276X-7-119

[30] Gangaja B, Chandrasekharan S, Vadukumpully S. Surface chemical analysis of CuO nanofiber composite electrodes at different stages of lithiation/delithiation. Journal of Power Sources. 2017;**340**:356-364. DOI: 10.1016/j.jpowsour.2016.11.087

[31] Pumera M, Iwai H, Miyahara Y. Germanium-oxide-coated carbon nanotubes. Nanotechnology. 2009;**20**:425606. DOI: 10.1088/0957-4484/20/42/425606

[32] John J, Gangaja B, Nair SV. Conformal coating of TiO2 shell on silicon nanoparticles for improved electrochemical performance in Li-ion battery applications. Electrochimica Acta. 2017;**235**:191-199. DOI: 10.1016/j.electacta.2017.03.127